

Yu.S. Dzyazko¹, V.M. Ogenko¹, L.Ya. Shtenberg², A.V. Bildyukevich³, T.V. Yatsenko¹

COMPOSITE ADSORBENTS INCLUDING OXIDIZED GRAPHENE: EFFECT OF COMPOSITION ON MECHANICAL DURABILITY AND ADSORPTION OF PESTICIDES

¹ *V.I. Vernadskii Institute of General and Inorganic Chemistry of National Academy of Sciences of Ukraine
32/34 Academician Palladin Avenue, Kyiv, 03142, Ukraine, E-mail: ogenko@gmail.com*

² *Scientific and Technical Institution "Institute of Chemical Technology and Industrial Ecology"*

³ *Chemist's Sq., Rubizhne, Lugans'k region, 93000, Ukraine*

³ *Institute of Physical Organic Chemistry of National Academy of Sciences of Belarus
13 Surganova Str., Minsk, 220072, Republic of Belarus*

A number of multifunctional composite adsorbents based on hydrated zirconium dioxide has been synthesized. The inorganic ion exchanger contained nanosheets of oxidized graphene (GO), the modifier amount was 0.5–7 mass %. The composites were investigated with methods of transmission electron microscopy and nitrogen adsorption-desorption, macropores were determined using water as a working liquid. It has been found that increasing of GO content depresses microporosity, but meso- and macroporosity grow. Crushing strength reduces exponentially with increase of total pore volume from 0.49 to 0.62 cm³ g⁻¹. Removal of phenol from water containing also inorganic ions was investigated. Adsorption capacity reaches 0.15–0.85 (phenol), 0.5–0.85 (Ca²⁺ and Mg²⁺), 0.005–0.045 (SO₄²⁻) mmol g⁻¹. When the GO content in the composites is 0.5–2 %, this carbon addition improves adsorption of cations and organic molecules comparing with hydrated zirconium dioxide. Further increase in GO amount causes no sufficient effect on adsorption due to decline of specific surface area of the composites. It has been suggested that the optimal content of the modifier, which provides the maximal growth of adsorption capacity, is 2 %. This composite is obtained in a form of large granules (0.3–0.5 mm), their crushing strength is 9 bar. The material was applied to removal of pesticides (acetomipride, carboxine, epoxyconazole and thiamethoxam) from aqueous multicomponent solution under batch conditions. The residual content of carboxine and epoxyconazole, molecules of which contain benzene rings, is lower than the maximal allowable concentration. No deterioration of pesticide uptake has been found after five cycles of adsorption-regeneration.

Keywords: *graphene oxide, hydrated zirconium dioxide, adsorption, phenol, pesticide, crushing strength*

INTRODUCTION

Graphene oxide (GO) and graphene-like materials are produced from graphite by means of aggressive chemical reagents, which provide its exfoliation, lamination and oxidation [1–3]. Nanosized flakes are obtained by this manner, their thickness is 0.54 nm, i.e. one atom (GO) or several nanometers (graphene-like materials). There are carboxyl groups along the flake perimeter, it is also valid for a part of phenolic groups. Other part of them as well as epoxy groups are located on different sides of the flake planes. The flakes form mechanically durable aggregates and agglomerates, the sheets forming by this manner are overlapped and curled. The capability of GO to aggregation allows one to obtain graphene paper [4, 5] and even membranes [6, 7].

These oxygen-containing groups provide hydrophilic properties of GO [8–10]. This is very

important for supercapacitors made of carbon materials [11–13], especially for the electrodes applied to capacitive deionization [14, 15]. Hydrophilicity is also significant for proton conductivity of graphene materials [16], and especially for adsorption.

GO is an effective adsorbent of inorganic ions, such as UO₂²⁺, from diluted nitrate solutions [17], where uranyl ions exist in cationic forms [18]. Adsorption reaches a maximum at pH 4–8, when both cationic and neutral uranyl complexes coexist in aqueous media [17]. Formation of inner-sphere complexes of U(VI) on GO surface has been proved. Ion exchange mechanism is suggested for Cu²⁺ adsorption, however, adsorption rate obeys kinetic equation of pseudo-second order [19] indicating chemical interaction of ions with GO surface. This interaction is similar for Cr³⁺, Pb²⁺, Cu²⁺, Cd²⁺, Ag⁺ ions, they destabilize GO suspension more

aggressively than Na^+ , K^+ and hardness ions [20]. As a result of destabilization, GO flakes form aggregates and agglomerates: 1D tubes, 2D multiple overlapped GO planes, and 3D sphere-like particles.

Regarding anion adsorption, GO shows practically no activity [10]. Nevertheless, adsorption of anionic azo-dyes are suggested [21], it is possible evidently due to interaction of benzene rings with hydrophobic regions of the carbon material. Hydrophobic porosity have been found experimentally [8–11, 22]. In order to form anion exchange capability of GO, it is functionalized with low molecular weight amines [23]. Such polyelectrolyte as cetyltrimethylammonium was also applied to functionalization [24]. Insoluble synthetic or natural polymers were used for preparation of GO-containing composites: polyethyleneimine [25], polyaniline [26], chitosan [27]. GO was also embedded to alginate beads [28]. Chromate [23–26, 28] and arsenate anions [27, 28] can be effectively removed from water using the obtained material. GO evidently increases surface area of the polymers facilitating adsorption of anions. For instance, a high capacity of $436 \text{ mg}\cdot\text{g}^{-1}$ toward Cr(VI) anions has been reported [25]. Both GO [29, 30] and GO-containing composites (based on calcium alginate [31] or natural polysaccharides [32–35]) can be applied to removal of cationic dyes from water. Exponential increase of dye uptake with oxidation degree of GO [29] indicates main contribution of its hydrophilic regions to adsorption.

Hydrophobic regions of GO are important for adsorption of molecular organic substances, such as tetracycline [36], aromatic (naphthalene, 1-naphthol) [37] and nitroaromatic compounds (*m*-dinitrobenzene, nitrobenzene, and *p*-nitrotoluene) [38], diclofenac and sulfamethoxazole [39], deoxyribonucleic acid (DNA) [40, 41], hormones [42]. Comparing with chemically reduced and annealing reduced graphene, adsorption capacity of GO towards binuclear aromatics is lower [37]. Similar regularity has been found for nitroaromatic compounds [38]. However, adsorption of Cd^{2+} on GO results in coadsorption of these organic compounds via surface-bridging mechanism, namely cation– π interaction [39]. The rate of DNA adsorption on GO is lower comparing with reduced GO, but desorption of this compound is considerable

[40]. Thus, it is possible to use this carbon material repeatedly.

Unfortunately practical application of GO materials in adsorption columns is difficult due to their small particle size, since such particles provide high hydrodynamical resistance under compaction, and easy removed from the column under loosening. In this case, a fine-porous filter for particles is necessary, this barrier produces additional resistance. Composites in a form of rather large lasting beads are more attractive from the technological point of view. Such inorganic adsorbents as oxides of multivalent metals correspond to this requirement. Oxide-based materials are amphoteric: they are capable to sorb both cations and anions [43]. Moreover, oxide nanoparticles can be formed during precipitation [10]. Thus, oxides of multivalent metals can be applied to modifying some functional materials: polymers for baromembrane separation [44, 45], inorganic membranes for electrodialysis [46, 47], ion exchange resins for sorption processes [48–50]. Insertion of GO into oxide matrices allows one to obtain multifunctional adsorbents: they are capable to sorb organic molecules as well as organic and inorganic cations [10]. The composites were applied to adsorption of cationic dye (the matrix was chitosan including magnetic particles) [51], particularly followed by photocatalytic degradation (the composite was based on TiO_2) [52], removal of Pb^{2+} , Hg^{2+} , and Cu^{2+} from water (Fe_3O_4 particles were a support) [53] and even for H_2S adsorption [54]. In the last case, the composite uptake is due to hydrated zirconium dioxide (HZD), which is characterized by developed surface (about $200 \text{ m}^2\cdot\text{g}^{-1}$). Larger value has been found in [10] ($\approx 350 \text{ m}^2\cdot\text{g}^{-1}$). Comparing with hydrated oxides of other multivalent metals [50], and even with zirconium hydrophosphate [55], the smallest primary particles are typical for HZD [50]. It is valid for precipitation from aqueous solutions of chloride salts in alkaline media under ambient conditions [50].

Earlier we investigated the composite containing GO obtained from graphite [10]. As found, the composite possesses both cation and anion exchange capability. It is also capable to sorb neutral organic molecules like phenol and lactose. At the same time, the question about the amount of carbon filler in this inorganic matrix is still opened. GO flakes loosen porous structure

of the HZD-based composite. This evidently enhances fragility of the adsorbent granules. Thus, the aim of the work was to find optimal composition of GO-containing adsorbents that provides high adsorption on the one hand and mechanical stability on the other hand.

Adsorption of some pesticides from water was investigated. Advanced commercial plant protection products show rather fast degradation in aqueous solutions under the influence of solar radiation. However, they are dangerous immediately after entering the environment [56–58]. Adsorption method of pesticide removal from water is often used, sometimes adsorption is accompanied by photodegradation [59]. The development of new effective adsorbents is an actual task.

EXPERIMENTAL

GO was obtained from commercial graphite ("Zaporizhskii graphit" LTD) using modified Hummer's method that involves H_2SO_4 , H_3PO_4 , KMnO_4 , H_2O_2 [1]. This technique was described earlier in detail, characterization of obtained material (XRD and IR spectroscopy, standard contact porosimetry) was also reported [10]. GO was obtained in a form of aqueous suspension (2.8 mg cm^{-3}).

The method for obtaining HZD xerogel and GO-containing composites based on this inorganic ion-exchanger was similar to [10]. The technique involved HZD precipitation from sol of insoluble zirconium hydroxocomplexes (one-component HZD) or suspension of GO in this sol (composite). In terms of anhydrous zirconium oxide, 100 cm^3 of sol contained 12.3 g ZrO_2 . Sol (100 cm^3) and GO suspension (22.5, 45, 90, 220, and 307 cm^3) were mixed. Just after ultrasonic activation of this mixture, the composite was precipitated with a saturated NaOH solution, washed with a $0.1 \text{ M NH}_4\text{OH}$ solution and deionized water, and dried. The material obtained by this manner contained 0.5, 1, 2, 5, and 7 mass. % of GO in relatively anhydrous ZrO_2 . The samples were marked as HZD-GO-0.5, HZD-GO-1 and so on.

Further the adsorbents were sieved, each fraction was weighted, the fraction of the largest mass was assumed as dominated. Granules of the samples were tested for crushing strength according to the State Standard [60] that is based on the Interstated Standard [61]. The measurements provide

investigations of 20 granules of each sample, their shape was maximally close to spherical. A MIP-10-1 device (USSR) was applied to the research. Visualization of the composite structure was carried out using a JEOL JEM 1230 transmission electron microscope (Jeol).

Micro- and mesopores of the adsorbents were determined by the method of nitrogen adsorption-desorption using a Quantachrome Autosorb 6B device (Quantachrome Instruments). Preliminarily the samples were degassed at 150°C during 2 h down to residual pressure of 0.7 mPa . The mass of each sample was 0.1 g . The isotherm data were calculated according to different methods. The volume and surface of micropores were determined using the Dubinin-Radushkevich (DR) algorithm, the parameters of mesopores were estimated by means of Barrett-Joyner-Halenda (BJH) approach.

In order to determine macropores, the samples were heated at 150°C for 2 h and weighted. A weighted sample were degassed as mentioned above. Then it was impregnated with water under vacuum, water was removed from the outer surface of grains with filter paper, then the sample was weighted again. The procedure was repeated until achievement of constant mass. The temperature was $20 \pm 2^\circ\text{C}$. The total volume of pores, which are occupied with water, was calculated taking into account the increase of the sample mass, and water density under this temperature. Total pore volume was obtained by this manner. The volume of macropores was calculated as a difference between the total pore volume and the volume corresponding to micro- and mesopores. IUPAC classification was taken into consideration (the size of micropores is less than 2 nm , this value is larger than 50 nm for macropores, the intermediate magnitudes correspond to mesopores).

For preliminary testing, solutions containing phenol ($70 \text{ mg}\cdot\text{dm}^{-3}$ or $0.74 \text{ mmol}\cdot\text{dm}^{-3}$) was prepared using tap water. Water contained divalent ions ($\text{mmol}\cdot\text{g}^{-1}$): Ca^{2+} (1.1), Mg^{2+} (0.5), SO_4^{2-} (0.42). The mass ratio of the adsorbent and solution was 1:500. The method of solution analysis before and after adsorption was based on the reaction between phenol, sodium nitroprusside and hydroxylamine hydrochloride in a buffer medium ($\text{pH } 10.6\text{--}11.8$) [62]. Sulphate ions were determined according to standard method [63]. The technique is based on

precipitation of SO_4^{2-} with BaCl_2 followed by dissolution of the precipitate with an EDTA solution in ammonia medium. Further the excess of EDTA was titrated with a Mg^{2+} -containing solution, Eriochrome Black T was used as an indicator. The method for analysis of hardness ions was based on the formation of the EDTA complexes [64]. Titration was performed at pH 10 (supported with NaOH) using Eriochrome Black T.

Some pesticides were applied to the study of adsorption properties of the composites. A mixed aqueous solution was prepared, it was a model of a diluted solution of commercial products. The solution contained acetomipride (AMP, $100 \text{ mg}\cdot\text{dm}^{-3}$), carboxine (CBX, $170 \text{ mg}\cdot\text{dm}^{-3}$), epoxyconazole (EPC, $70 \text{ mg}\cdot\text{dm}^{-3}$) and thiamethoxam (TMT, $100 \text{ mg}\cdot\text{dm}^{-3}$) (Fig. 1). Then the solution was diluted in 200, 50, 20, 10, 3.3, 2 and 1.3 times. These solutions were applied to obtaining adsorption isotherms.

The ratio of the masses of adsorbent and solution was 1:100, the time of contact was 48 h. The solution samples were taken periodically and analyzed using an Agilent 1290 liquid chromatograph supplied with an Agilent 6400 triple quadrupole detector (Agilent). The value of adsorption capacity (A) was calculated via:

$$A = \frac{(C_0 - C)V}{m}, \quad (1)$$

where C_0 and C are the initial and residual concentration respectively, V is the solution volume, m is the adsorbent mass.

After adsorption from the most diluted solution, the HZD-GO-1 sample was boiled in a 0.1 M NaOH solution for 1 h, washed with deionized water down to neutral reaction of the effluent and used again for pesticide recovery from water. This procedure was repeated several times.

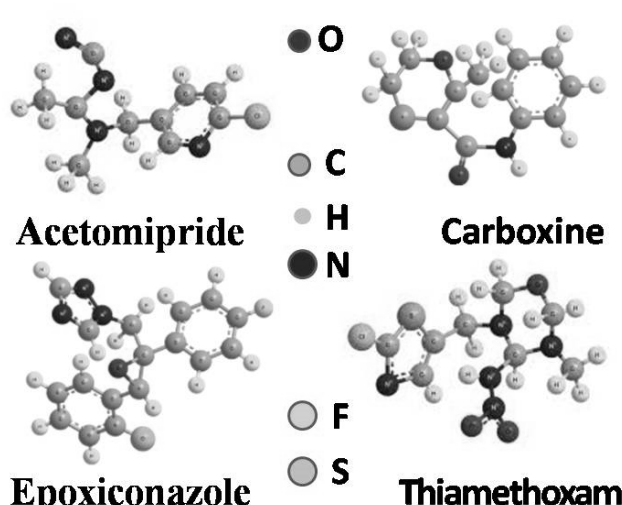


Fig. 1. Organic compounds used for adsorption investigations

RESULTS AND DISCUSSION

Since sol of insoluble zirconium hydroxocomplexes contained mainly nanoparticles (6 nm [10]), they could be visible in TEM image. However, the inorganic nanoparticles are adsorbed by GO nanosheets. When HZD is precipitated, the nanoparticles are aggregated forming larger particles ($\approx 30\text{--}200 \text{ nm}$) of irregular shape (Fig. 2). Zr–O–Zr bonds at the contact points of the primary nanoparticles prevent the of aggregate fragmentation. Nevertheless, the primary HZD nanoparticles

cannot be recognized with a TEM method, since they are coated with GO. As found earlier, HZD-GO composite contains three types of particles: (i) HZD particles coated with GO nanosheets, (ii) HZD particles that are free from GO, (iii) aggregates of GO nanosheets [10]. A growth of the GO content evidently reduces the amount of the particles of the second type. Simultaneously the contribution of the particles of the first and third types increases. Screening of HZD surface with GO nanosheets prevents cross-linkage of HZD particles. As a result,

smaller granules are formed comparing with one-component HZD (Table 1).

GO affects porous structure of HZD matrix. Fig. 3 illustrates typical isotherm of nitrogen adsorption and desorption. According to the IUPAC classification, the isotherm is related to the 1st type (similarly to Langmuir isotherm)

[65]. It is convex relatively to the abscissa axes, and shows rapid growth in the region of low P/P_s . A wide plateau is also observed. The isotherm shows no hysteresis, it is characteristic for the curves of the 1st type attributed to microporous materials.

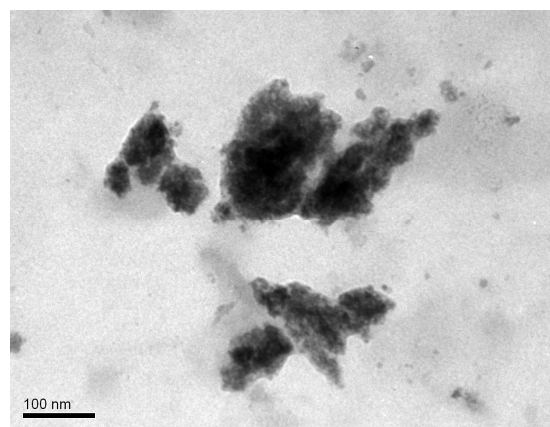


Fig. 2. TEM image of HZD-GO-5

Table 1. Granule size and data of porometric measurements

Sample	Dominated fraction, mm	Pore volume, cm^3g^{-1}			Surface area, m^2g^{-1}	
		micropores	mesopores	macropores		
HZD	0.50–0.80	0.11	0.02	0.36	0.49	338
HZD-GO-0.5	0.25–0.50	0.10	0.02	0.38	0.50	320
HZD-GO-1	0.25–0.50	0.10	0.03	0.42	0.55	311
HZD-GO-2	0.25–0.50	0.09	0.03	0.44	0.56	296
HZD-GO-5	0.10–0.25	0.08	0.04	0.47	0.59	285
HZD-GO-7	<0.10	0.08	0.05	0.49	0.62	281

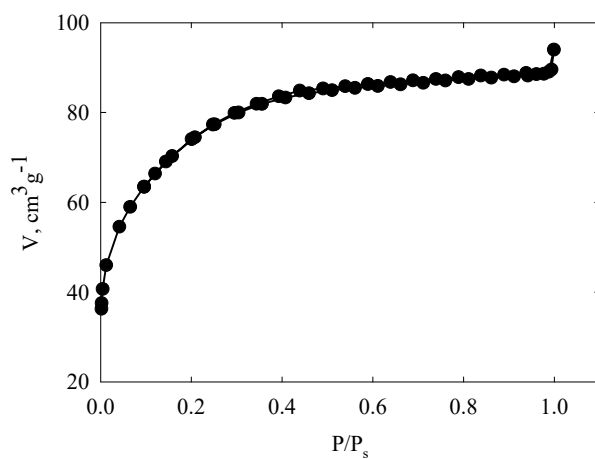
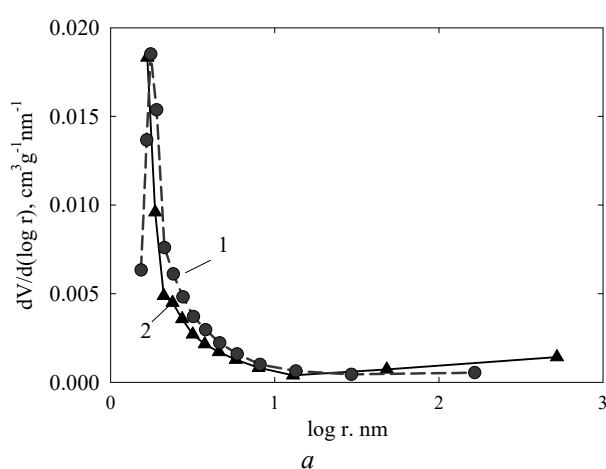


Fig. 3. Isotherms of nitrogen adsorption-desorption for HZD-GO-2 sample. This type of isotherms is characteristic both for one-component HZD and other GO-containing composites

Differential pore size distributions for HZD demonstrate a sharp peak at pore radius (r) of 1.8 nm (Fig. 4). The material is practically non-porous in the region of 10–100 nm. This is in agreement with the data obtained by means of the method of standard contact porosimetry [10]. Increasing in GO content depresses microporosity but enhances meso- and macroporosity. This is evidently caused by loosening HZD particles due to GO nanosheets on their surface. Indeed, the blurred maxima are visible on the pore distributions after the intensive sharp peaks near $r = 1.5$ nm. Within the framework of geometrical globular model, it means the alternation of pores between HZD globules: pore necks (smaller pores) and pore cavities (larger pores) [66]. Moreover, GO nanosheets can also contribute to meso- and macroporosity. At the same time, microporosity

decreases probably due to coalescence of HZD micropores affected by GO, and their transformation to mesopores.

The values of specific surface area for the pristine HZD and HZD-GO-2 are smaller than those obtained by the method of standard contact porosimetry [10]. For instance, the magnitude of $\approx 380 \text{ m}^2 \cdot \text{g}^{-1}$ (HZD) has been found for these samples in aqueous medium. In the case of HZD, higher value of specific surface area is due to hydration of $=\text{Zr}-\text{OH}$ groups (water is partially removed from the hydration shells of counterions during thermal pretreatment). It is also the same for functional groups attributed to GO. Moreover, water or octane wet GO penetrating between graphene sheets. As a result, cavities are formed (they are unavailable for nitrogen adsorption) [9].



a

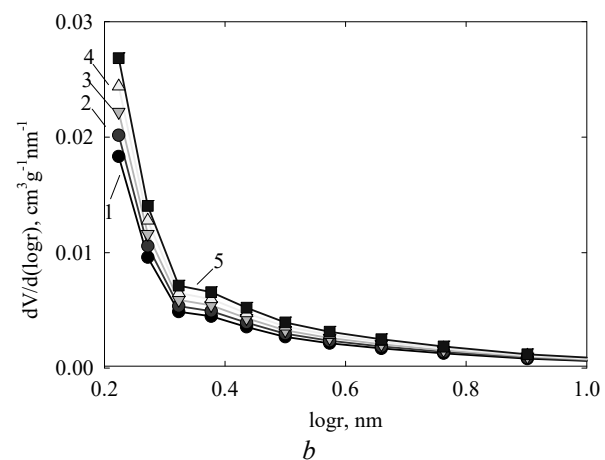


Fig. 4. Differential pore size distributions in different scales: *a* – HZD (1), HZD-GO-0.5 (2); *b* – HZD-GO-0.5 (1), HZD-GO-1 (2), HZD-GO-2 (3), HZD-GO-5 (4), HZD-GO-7 (5)

Regarding HZD and HZD-GO-2 samples, the values of total pore volume per mass unit are in agreement with the data obtained by the method of standard contact porosimetry [10]. In general, these magnitudes grow with increase in GO content. Porosity affects mechanical durability of the composites, namely crushing strength, σ (Fig. 5 *a*). This parameter reduces with increase of porosity (*i.e.* with increase in GO content). This dependence can be fitted with an exponential decay function:

$$\sigma = \sigma_0 e^{-bV}, \quad (2)$$

where σ_0 is the effective value of a non-porous material (it is assumed that no change of crushing strength is affected by GO), b is the constant ($b = 3.8 \text{ g} \cdot \text{cm}^{-3}$). Extrapolation of the curve to the ordinate axis gives the value of 7.8 MPa. It is easy to obtain from eq. (2):

$$\ln \frac{\sigma}{\sigma_0} = -bV. \quad (3)$$

Linearization of function (2) gives a straight line (Fig. 5 *b*). Normally a linear polynomial contains also additional constant a , *i.e.*

$\ln \frac{\sigma}{\sigma_0} = a - bV$. In our case, $a = 0.05$, the a value is close to 0. In fact, equ. (3) is similar to Archie equation for electrical conductivity [67]. This type of function is typical for dependences of mechanical characteristics on porosity (pore

volume per volume unit) [68]. The b constant depends on shape of pores, their anisotropy, tortuosity etc. In our case, it is difficult to determine the volume porosity, since the adsorbents are dispersed.

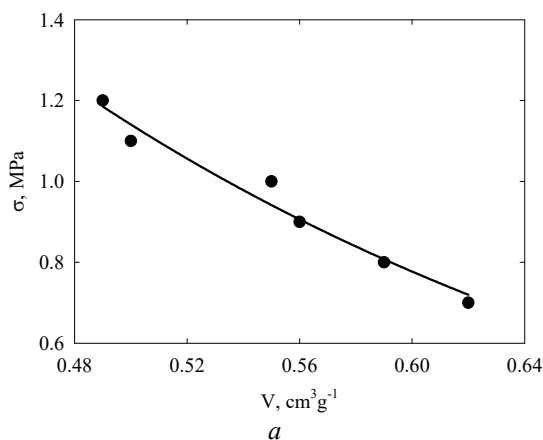
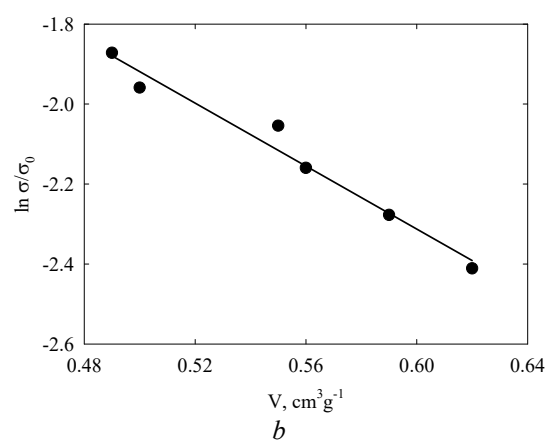
*a**b*

Fig. 5. Dependences of crushing strength (*a*) and $\ln(\sigma/\sigma_0)$ (*b*) on pore volume of HZD-GO composites

GO affects also adsorption properties of the composites. As seen from Fig. 6, GO improves adsorption of hardness ions. This improvement is considerable up to the GO content of 2 mass. %. No sufficient growth of adsorption capacity is observed, when the content of this carbon addition is higher. It is the same for phenol adsorption. HZD shows practically no capability to sorb organic species. Indeed, phenol is a weak acid, the pH of equilibrium solutions was about 4 due to preferable cation exchange. Phenol molecules are not dissociated under these conditions.

The plateau of the curve for Ca^{2+} and Mg^{2+} ions is probably due to competing factors: increase of the content of ion exchange groups ($-\text{COOH}$) on the one hand and decrease of specific surface area on the other hand. The last factor also depresses anion exchange (SO_4^{2-} adsorption). Other reason of the lower anion adsorption is screening HZD surface with GO nanosheets (GO shows only cation exchange capability). Regarding phenol adsorption, the plateau is also observed due to decrease of surface area on the one hand and enhancement of the composite hydrophobicity on the other hand.

The obtained results allowed us to choose the composite containing 2 % of GO for further investigations. First of all, no sufficient increase

of adsorption capacity has been found for the samples with higher content of this carbon material. As opposed to HZD-GO-5 and HZD-GO-7, the HZD-GO-2 sample is characterized by higher mechanical durability against crushing. It also possesses higher anion exchange capacity. Moreover, larger granules can be obtained during precipitation from the suspension containing insoluble zirconium hydroxocomplexes and GO. Based on this approach, adsorption of pesticides on the composite containing 2 % of GO was studied.

Fig. 7 illustrates the residual concentration of organic compounds in water after adsorption. These data are plotted as functions of initial concentration. When the initial EPX concentration was $0.35 \text{ mg} \cdot \text{dm}^{-3}$, it was possible to reduce its content below the maximal allowable concentration (MAC). The initial concentration of this substance was the lowest among the studied pesticides. At the same time, there was the highest content of CBX in the multicomponent solution. Nevertheless, it is possible to reduce its content below the MAC at $C_0 = 0.85-8.5 \text{ mg} \cdot \text{dm}^{-3}$. When the initial concentration of AMP and TMX was the lowest, the residual content was higher than MAC. However, the C and MAC values are the magnitudes of the same order.

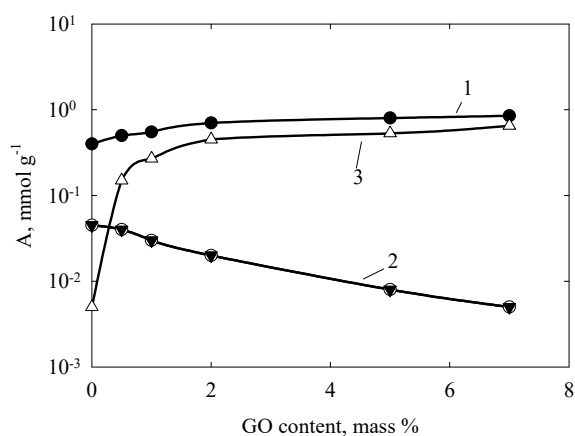


Fig. 6. Adsorption capacity of the composites as a function of GO content. Species: hardness ions (1), SO_4^{2-} (2), phenol (3)

Based on the obtained results, adsorption capacity of the composites has been calculated (Fig. 8 a). The isotherm for CBX is characterized by rapid growth in the region of low concentration. Further its growth becomes slower: the curve tends to plateau. Some retardation of the capacity growths is also visible for EPX. This tendency is most expressed for AMP and TMX. However, the isotherms show rapid growth again in the region of high concentration. This indicates polymolecular adsorption.

A number of models were applied to the isotherms. The best results were achieved, when the curves were calculated according to the Langmuir model (Fig. 8 b), the data for polymolecular adsorption were omitted (AMP and TMX). The calculations were performed via [69]:

$$\frac{1}{A} = \frac{1}{K_L A_L C} + \frac{1}{A_L}, \quad (4)$$

where is A_L the monolayer capacity, K is the constant that characterizes the energy of interaction with surface. The calculated data are given in Table 2. The largest Langmuir constants have been found for EPX, the lowest values have been estimated for TMX. CBX and TMX, which are characterized by the weakest interaction with the composite surface, are adsorbed most quickly: more than $\approx 50\%$ of toxic components are removed during the first

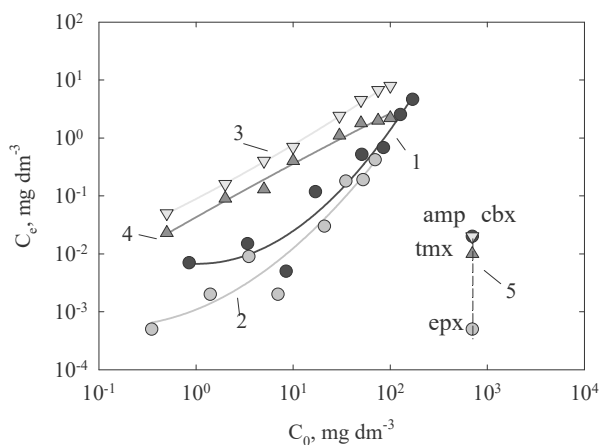


Fig. 7. Residual concentration of pesticides in multicomponent solutions as a function of their initial concentration. Pesticides: CBX (1), EPX (2), AMP (3), TMX (4), maximal allowed concentration (5)

hour. Nevertheless, adsorption capacity is close to the equilibrium data after 18 h for all organic substances.

It should be noted that the largest values of adsorption capacity has been found for EPX – its molecules include 2 benzene rings. Lower magnitudes were found for CBX (1 benzene ring). Weaker adsorption is typical for AMP (one heterocyclic ring). At last, TMX (two heterocyclic rings) shows the most inconsiderable adsorption. In the case of inactivated biochar, which contains mainly non-graphitized carbon, CBX is adsorbed preferably from the solution containing also TMX and AMP, TMX is worse adsorbed than AMP [70]. It is possible to assume that benzene rings promote adsorption of organic compounds on carbon materials, heterocycles depress adsorption.

The possibility of multiple use of the composite were investigated. As known, the mentioned pesticides are hydrolytically stable up to pH 9, degradation occurs in alkaline media [71]. Thus, alkaline solutions were used for the composite regeneration. After regeneration with alkaline solution that provides destruction of pesticides, no deterioration of adsorption has been found (Table 3). Dissociation of functional groups is enhanced in alkaline media ($=\text{Zr}-\text{OH}$ groups of HZD, carboxyl and phenolic groups of GO). The surface charge evidently prevents adsorption of the products of pesticide destruction.

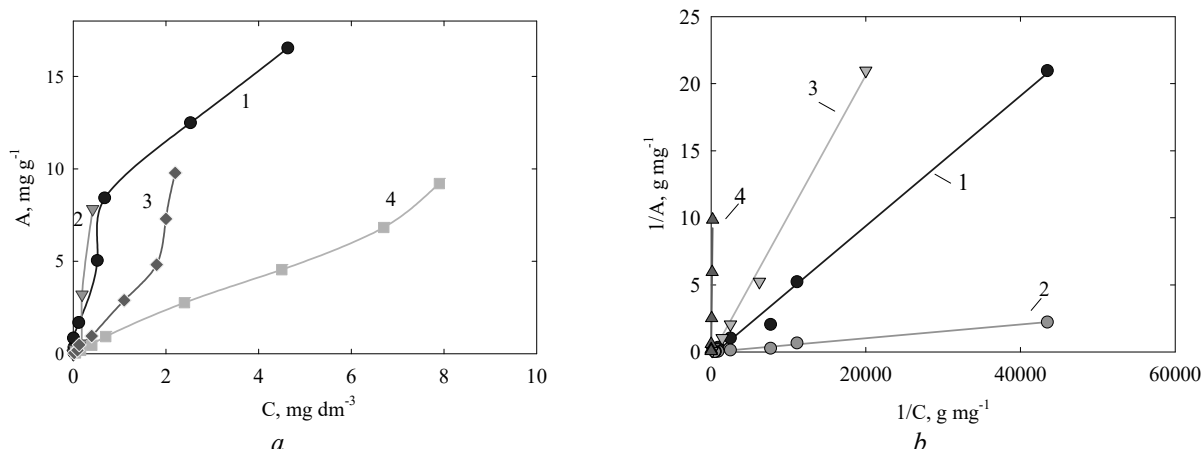


Fig. 8. Isotherms of pesticide adsorption on HZD-GO-2 sample plotted in ordinary (*a*) and Langmuir (*b*) coordinates. Pesticides: CBX (1), EPX (2), AMP (3), TMX (4)

Table 2. Pesticide adsorption on HZD-GO-2 sample

Pesticide	Molecular mass	Formula	Langmuir constants		$A \times 10^4, \text{mmol g}^{-1}$ (adsorption from the most diluted solution)			
			$A_L, \text{mg g}^{-1}$ (mmol g^{-1})	$K_L, \text{g mg}^{-1}$	1 h	5 h	18 h	48 h
CBX	235	$\text{C}_{12}\text{H}_{13}\text{NO}_2\text{S}$	16.9 (0.070)	59	1.26	2.95	3.48	3.57
EPX	330	$\text{C}_{17}\text{H}_{13}\text{ClF}_3\text{NO}$	71.1 (0.215)	281	9.95	16.9	18.8	19.13
AMP	223	$\text{C}_{10}\text{H}_{11}\text{ClN}_4$	8.4 (0.037)	245	0.85	1.51	1.85	2.02
TMX	292	$\text{C}_8\text{H}_{10}\text{ClNO}_3\text{S}$	4.7 (0.016)	6.7	0.94	1.32	1.55	1.58

Table 3. Multiple usage of HZD-GO-2 for removal of pesticides from water

Cycle number	$A \times 10^4$ (after adsorption from the most diluted solution), mmol g^{-1}			
	CBX	EPX	AMP	TMX
1	3.57	19.13	2.02	1.58
2	3.48	18.91	2.05	1.60
3	3.61	18.95	1.93	1.55
4	3.50	19.14	2.00	1.58
5	3.55	19.01	2.05	1.56

CONCLUSIONS

Among the composites containing 0.5–7 % GO, the HZD-GO-2 sample is the most attractive, since it possesses a complex of necessary functional properties. This material can be obtained in a form of rather large granules (0.3–0.5 mm), moreover, it is characterized by significant mechanical durability (the crushing strength is 9 bar). This gives a possibility to use the composite in adsorption columns. The adsorbent shows not only considerable capacity towards hardness ions in neutral media, but also the capability to adsorb anions. Moreover, the material is capable to adsorb

such toxic organic substances as phenol and a number of pesticides. When organic molecules contain benzene rings, it is possible to reduce their concentration below the maximal allowable concentration.

Increasing in GO content deteriorates mechanical durability of the composites based on HZD due to porosity growth. Small granules are formed during synthesis. At the same time, the composites demonstrate in sufficient growth of adsorption of inorganic cations and organic molecules. Significant depression of anion adsorption has been also found.

The HZD-GO-2 composite can be recommended as a multifunctional adsorbent to remove inorganic ions (both toxic species and hardness ions) and toxic organic compounds. Other possible field of adsorbent application is modifying of polymer and ceramic materials for baro- or electromembrane separation similarly to [44–47, 72].

ACKNOWLEDGEMENTS

The work was performed within the framework of the projects entitled

"Developments of materials and processes for removal of valuable and toxic components from the solutions of biogenic and technogenic origin" (supported by the NAS of Ukraine) and "Development of composite ultra- and microfiltration membranes with predetermined functional properties for complex processing of wastes of food industry" (supported by the NAS of Ukraine and NAS of the Republic of Belarus, grant numbers 0118U006245, X18UKA-021).

Композиційні адсорбенти, які включають окиснений графен: вплив складу на механічну міцність та адсорбцію пестицидів

Ю.С. Дзязько, В.М. Огенко, Л.Я. Штейнберг, О.В. Більдюкович, Т.В. Яценко

*Інститут загальної та неорганічної хімії ім. В.І. Вернадського Національної академії наук України
просп. Академіка Палладіна, 32/34, Київ, 03142, Україна, dzyazko@gmail.com*

*Науково-технічна установа "Інститут хімічної технології та промислової екології"
пл. Хіміків, 3, Рубіжне, Луганська область, 93000, Україна*

*Інститут фізико-органічної хімії Національної академії наук Білорусі
бул. Сурганова, 13, Мінськ, 220072, Республіка Білорусь*

Синтезовано ряд багатофункціональних композитних адсорбентів на основі гідратованого діоксиду цирконію. Неорганічний іоніт містив наночастинки окисненого графену (ОГ), кількість модифікатора становила 0.5–7 мас. %. Композити досліджували методами трансмісійної електронної мікроскопії та адсорбції–десорбції азоту. Встановлено, що збільшення вмісту ОГ призводить до зменшення мікропористості, при цьому зростає мезо- та макропористість, а загальний об'єм пор збільшується з 0.49 до 0.62 см³ г⁻¹. Міцність на розчавлювання експоненціально зменшується зі збільшенням об'єму пор. Досліджено вилучення фенолу з водопровідної води. Показано, що адсорбційна ефективність досягає 0.15–0.85 (фенол), 0.5–0.85 (Ca²⁺ i Mg²⁺), 0.005–0.045 (SO₄²⁻) ммоль г⁻¹. Коли вміст ОГ в композитах становить 0.5–2 %, ця вуглецева добавка покращує адсорбцію катіонів і органічних молекул у порівнянні з гідратованим діоксидом цирконію. Подальше збільшення кількості ОГ істотно не впливає на адсорбцію внаслідок зменшення питомої площині поверхні композитів. Стверджується, що оптимальний вміст модифікатора, що забезпечує максимальний приріст адсорбції, становить 2 %. Цей композит отримано у вигляді великих гранул (0.3–0.5 мм), їхня міцність на розчавлювання становить 9 атм. Матеріал використовували для видалення пестицидів (ацетомітріду, карбоксину, епоксіконазолу і тіаметоксаму) з водного багатокомпонентного розчину в статичних умовах. Залишковий вміст карбоксину і епоксіконазолу, молекули яких містять бензольні кільця, нижче гранично допустимої концентрації. Близько 50 % токсичних речовин видаляються протягом першої години. Після п'яти циклів адсорбції–регенерації не було виявлено погіршення адсорбції пестицидів.

Ключові слова: оксид графену, гідратований діоксид цирконію, адсорбція, фенол, пестицид, міцність на розчавлювання

Композиционные адсорбенты, включающие окисленный графен: влияние состава на механическую прочность и адсорбцию пестицидов

Ю.С. Дзынько, В.М. Огенко, Л.Я. Штейнберг, А.В. Бильдюкович, Т.В. Яценко

Институт общей и неорганической химии им. В.И. Вернадского Национальной академии наук Украины

просп. Академика Палладина, 32/34, Киев, 03142, Украина, dzyazko@gmail.com

Научно-техническое учреждение "Институт химической технологии и промышленной экологии"

пл. Химиков, 3, Рубежное, Луганская область, 93000, Украина

Институт физико-органической химии Национальной академии наук Беларусь

ул. Сурганова, 13, Минск, 220072, Республика Беларусь

Синтезирован ряд многофункциональных композитных адсорбентов на основе гидратированного диоксида циркония. Неорганический ионит содержал наночастицы окисленного графена (ОГ), количество модификатора составляло 0.5–7 масс. %. Композиты исследовали методами трансмиссионной электронной микроскопии и адсорбции-десорбции азота. Установлено, что увеличение содержания ОГ приводит к уменьшению микропористости, при этом возрастает мезо- и макропористость, а общий объем пор увеличивается с 0.49 до 0.62 см³ г⁻¹. Прочность на раздавливание уменьшается экспоненциально с увеличением объема пор. Исследовано извлечение фенола из воды. Показано, что адсорбционная емкость достигает 0.15–0.85 (фенол), 0.5–0.85 (Ca²⁺ и Mg²⁺), 0.005–0.045 (SO₄²⁻) ммоль г⁻¹. Когда содержание ОГ в композитах составляет 0.5–2 %, эта углеродная добавка улучшает адсорбцию катионов и органических молекул по отношению к гидратированному диоксиду циркония. Дальнейшее увеличение количества ОГ не оказывает существенного влияния на адсорбцию вследствие уменьшения площади удельной поверхности композитов. Утверждается, что оптимальное содержание модификатора, обеспечивающего максимальный прирост адсорбции, составляет 2 %. Этот композит получен в виде крупных гранул (0.3–0.5 мм), их прочность на раздавливание составляет 9 атм. Материал использовали для удаления пестицидов (ацетомиприда, карбоксина, эпоксионазола и тиаметоксама) из водного многокомпонентного раствора в статических условиях. Остаточное содержание карбоксина и эпоксионазола, молекулы которых содержат бензольные кольца, ниже максимально допустимой концентрации. Около 50 % токсичных веществ удаляются в течение первого часа. После пяти циклов адсорбции-регенерации не было обнаружено ухудшения адсорбции пестицидов.

Ключевые слова: оксид графена, гидратированный диоксид циркония, адсорбция, фенол, пестициды, прочность на раздавливание

REFERENCES

1. Marcano D.C., Kosynkin D.V., Berlin J.M., Sinitskii A., Sun Z., Slesarev A., Alemany L.B., Lu W., Tour J.M. Improved synthesis of graphene oxide. *ACS Nano*. 2010. **4**(8): 4806.
2. Stankovich S., Piner R.D., Nguyen S.B.T., Ruoff R.S. Synthesis and exfoliation of isocyanate-treated graphene oxide nanoplatelets. *Carbon*. 2006. **44**(15): 3342.
3. Chen J., Yao B., Li Ch., Shi G. An improved Hummers method for eco-friendly synthesis of graphene oxide. *Carbon*. 2013. **64**: 225.
4. Tao L.-C., Zhang K.-N., Tian H., Liu Y., Wang D.-Y., Chen Y.-Q., Yang Y., Ren T.-L. Graphene-paper pressure sensor for detecting human motions. *ACS Nano*. 2017. **11**(9): 8790.
5. Yao Y., Jiang Ch., Ping J. Flexible freestanding graphene paper-based potentiometric enzymatic aptasensor for ultrasensitive wireless detection of kanamycin. *Biosens. Bioelectron*. 2019. **123**: 178.
6. Tan P., Sun J., Hu Y., Fang Z., Bi Q., Chen Y., Cheng J. Adsorption of Cu²⁺, Cd²⁺ and Ni²⁺ from aqueous single metal solutions on graphene oxide membranes. *J. Hazard. Mater.* 2015. **297**: 251.
7. Joshi R.K., Alwarappan S., Yoshimura M., .Sahajwalla V., Nishina Y. Graphene oxide: the new membrane material. *Appl. Mater. Today*. 2015. **1**(1): 1.
8. Volkovich Y.M., Lobach A.S., Spitsyna N.G., Baskakov S.A., Sosenkin V.E., Rychagov A.Y., Kabachkov E.N., Sakars A., Michtchenko A., Shulga Y.M. Hydrophilic and hydrophobic pores in reduced graphene oxide aerogel. *J. Porous Mater.* 2019. **26**(4): 1111.

9. Volkovich Y.M., Rychagov A.Y., Sosenkin V.E., Efimov O.N., Os'makov M.I. Measuring the specific surface area of carbon nanomaterials by different methods. *Russ. J. Electrochim.* 2014. **50**(11): 1099.
10. Dzyazko Yu.S., Ogenko V.M., Volkovich Yu.M., Sosenkin V.E., Maltseva T.V., Yatsenko T.V., Kudelko K.O. Composite consisting of hydrated zirconium dioxide and graphene oxide for removal of organic and inorganic components from water. *Him. Fiz. Technol. Poverhni.* 2018. **9**(4):417.
11. Shulga Y.M., Baskakov S.A., Baskakova Y.V., Volkovich Y.M., Shulga N.Y., Skryleva E.A., Parkhomenko Y.N., Belay K.G., Gutsev G.L., Rychagov A.Y., Sosenkin V.E., Kovalev I.D. Supercapacitors with graphene oxide separators and reduced graphite oxide electrodes. *J. Power Sources.* 2015. **279**: 722.
12. Shulga Y.M., Baskakov S.A., Baskakova Y.V., Lobach A.S., Kabachkov E.N., Volkovich Y.M., Sosenkin V.E., Shulga N.Y., Nefedkin S.I., Kumar Y., Michtchenko A. Preparation of graphene oxide-humic acid composite-based ink for printing thin film electrodes for micro-supercapacitors. *J. Alloys Compd.* 2018. **730**: 88.
13. Volkovich Yu.M., Mazin V.M., Urisson N.A. Operation of double-layer capacitors based on carbon materials. *Russ. J. Electrochim.* 1998. **34**(8): 740.
14. Volkovich Y., Bograchev D., Mikhlin A., Rychagov A., Sosenkin V., Milyutin V., Park D. Electrodes based on carbon nanomaterials: structure, properties, and application to capacitive deionization in static cells. *Springer Proceedings in Physics.* 2018. **210**: 127.
15. Volkovich Y.M., Bograchev D.A., Mikhlin A.A., Rychagov A.Y., Sosenkin V.E., Park D. Capacitive deionization of aqueous solutions: modeling and experiments. *Desalin. Water Treat.* 2017. **69**: 130.
16. Smirnov V.A., Denisov N.N., Dremova N.N., Volkovich Y.M., Rychagov A.Y., Sosenkin V.E., Belay K.G., Gutsev G.L., Shulga N.Yu., Shulga Y.M. A comparative analysis of graphene oxide films as proton conductors. *Appl. Phys. A.* 2014. **117**(4): 1859.
17. Li Z., Chen F., Yuan L., Liu Y., Zhao Y., Chai Z., Shi W. Uranium(VI) adsorption on graphene oxide nanosheets from aqueous solutions. *Chem. Eng. J.* 2012. **210**: 539.
18. Gapel G. Speciation of actinides. In: *Handbook of elemental speciation II. Species in the environment, food, medicine and occupational health* (Chichester, UK: Wiley, 2005).
19. Mi X., Huang G., Xie W., Wang W., Liu Y., Gao J. Preparation of graphene oxide aerogel and its adsorption for Cu²⁺ ions. *Carbon.* 2012. **50**(13): 4856.
20. Yang K., Chen B., Zhu X., Xing B. Aggregation, adsorption, and morphological transformation of graphene oxide in aqueous solutions containing different metal cations. *Environ. Sci. Technol.* 2016. **50**(20): 11066.
21. Konicki W., Aleksandrzak M., Moszyński D., Mijowska E. Adsorption of anionic azo-dyes from aqueous solutions onto graphene oxide: Equilibrium, kinetic and thermodynamic studies. *J. Colloid Interface Sci.* 2017. **496**: 188.
22. Shulga Y.M., Baskakov S.A., Baskakova Y.V., Lobach A.S., Volkovich Y.M., Sosenkin V.E., Shulga N.Y., Parkhomenko Y.N., Michtchenko A., Kumar Y. Hybrid porous carbon materials derived from composite of humic acid and graphene oxide. *Microporous Mesoporous Mater.* 2017. **245**: 24.
23. Kumar A.S.K., Kakan S.S., Rajesh N. A novel amine impregnated graphene oxide adsorbent for the removal of hexavalent chromium. *Chem. Eng. J.* 2013. **230**: 328.
24. Wu Y., Luo H., Wang H., Wang C., Zhang J., Zhang Z. Adsorption of hexavalent chromium from aqueous solutions by graphene modified with cetyltrimethylammonium bromide. *J. Colloid Interface Sci.* 2013. **394**: 183.
25. Geng J., Yin Y., Liang Q., Zhu Z., Luo H. Polyethyleneimine cross-linked graphene oxide for removing hazardous hexavalent chromium: Adsorption performance and mechanism. *Chem. Eng. J.* 2019. **361**: 1497.
26. Ansari M.O., Kumar R., Ansari S.A., Ansari S.P., Barakat M.A., Alshahri A., Cho M.H. Anion selective pTSA doped polyaniline@graphene oxide-multiwalled carbon nanotube composite for Cr(VI) and Congo red adsorption. *J. Colloid Interface Sci.* 2017. **496**: 407.
27. Kumar A.S.K., Jiang S.J. Chitosan-functionalized graphene oxide: A novel adsorbent an efficient adsorption of arsenic from aqueous solution. *J. Environ. Chem. Eng.* 2016. **4**(2): 1698.
28. Vu H.C., Dwivedi A.D., Le T.T., Seo S.-H., Kim E.-J., Chang Y.-S. Magnetite graphene oxide encapsulated in alginate beads for enhanced adsorption of Cr(VI) and As(V) from aqueous solutions: role of crosslinking metal cations in pH control. *Chem. Eng. J.* 2017. **307**: 220.
29. Yan H., Tao X., Yang Z., Li K., Yang H., Li A., Cheng R. Effects of the oxidation degree of graphene oxide on the adsorption of methylene blue. *J. Hazard. Mater.* 2014. **268**: 191.
30. Robati D., Rajabi M., Moradi O., Najafi F., Tyagi I., Agarwal S., Gupta V.K. Kinetics and thermodynamics of malachite green dye adsorption from aqueous solutions on graphene oxide and reduced graphene oxide. *J. Mol. Liq.* 2016. **214**: 259.
31. Li Y., Du Q., Liu T., Sun J., Wang Y., Wu S., Wang Z., Xia Y., Xia L. Methylene blue adsorption on graphene oxide/calcium alginate composites. *Carbohydr. Polym.* 2013. **95**(1): 501.

32. Qi Y., Yang M., Xu W., He S., Men Y. Natural polysaccharides-modified graphene oxide for adsorption of organic dyes from aqueous solutions. *J. Colloid Interface Sci.* 2015. **486**: 84.
33. González J.A., Villanueva M.E., Piehl L.I., Copello G.J. Development of a chitin/graphene oxide hybrid composite for the removal of pollutant dyes: Adsorption and desorption study. *Chem. Eng. J.* 2015. **280**: 41.
34. Dai H.L., Huang Y., Huang H. Eco-friendly polyvinyl alcohol/carboxymethyl cellulose hydrogels reinforced with graphene oxide and bentonite for enhanced adsorption of methylene blue. *Carbohydr. Polym.* 2018. **185**: 1.
35. Li Z., Tan W.-Z., Liu X.-H., Sun Z.-F., Ren P.-G., Yan D.-X. Facile preparation of 3D regenerated cellulose/graphene oxide composite aerogel with high-efficiency adsorption towards methylene blue. *J. Colloid Interface Sci.* 2018. **532**: 58.
36. Gao Y., Li Y., Zhang L., Huang H., Hu J., Shah S.M., Su X. Adsorption and removal of tetracycline antibiotics from aqueous solution by graphene oxide. *J. Colloid Interface Sci.* 2012. **368**(1): 540.
37. Wang H., Chen P. Adsorption and coadsorption of organic pollutants and a heavy metal by graphene oxide and reduced graphene materials. *Chem. Eng. J.* 2015. **281**: 379.
38. Chen X., Chen B. Microscopic and spectroscopic investigations of the adsorption of nitroaromatic compounds on graphene oxide, reduced graphene oxide, and graphene nanosheets. *Environ. Sci. Technol.* 2015. **49**(10): 6181.
39. Nam S.W., Jung C., Li H., Yu M., Flora J.R.V., Boateng L.K., Her N., Zoh K.-D., Yoon Y. Adsorption characteristics of diclofenac and sulfamethoxazole to graphene oxide in aqueous solution. *Chemosphere.* 2015. **136**: 20.
40. Liu B., Salgado S., Maheshwari V., Liu J. DNA adsorbed on graphene and graphene oxide: Fundamental interactions, desorption and applications. *Curr. Opin. Colloid Interface Sci.* 2016. **26**: 41.
41. Lu C., P.-J.J. Huang, Liu B., Ying Y., Liu J. Comparison of graphene oxide and reduced graphene oxide for DNA adsorption and sensing. *Langmuir.* 2016. **32**(41): 10776.
42. Jiang L.-H., Liu Y.-G., Zeng G.-M., Xiao F.-Y., Hu X.-J., Hu X., Wang H., Li T.-T., Zhou L., Tan X.-F. Removal of 17 β -estradiol by few-layered graphene oxide nanosheets from aqueous solutions: External influence and adsorption mechanism. *Chem. Eng. J.* 2014. **284**: 93.
43. Amphlett C.B. *Inorganic Ion Exchangers.* (Amsterdam: Elsevier, 1964).
44. Myronchuk V.G., Dzyazko Yu.S., Zmievskii Yu.G., Ukrainets A.I., Bildukovich A.V., Kornienko L.V., Rozhdestvenskaya L.M., Palchik A.V. Organic-inorganic membranes for filtration of corn distillery. *Acta Periodica Technologica.* 2016. **47**: 153.
45. Zmievskii Yu., Rozhdestvenska L., Dzyazko Yu., Kornienko L., Myronchuk V., Bildukovich A., Ukrainetz A. Organic-inorganic materials for baromembrane separation. *Springer Proc. Phys.* 2017. **195**: 675.
46. Dzyazko Yu., Rozhdestveskaya L., Zmievskii Yu., Zakharov V., Myronchuk V. Composite inorganic anion exchange membrane for electrodialytic desalination of milky whey. *Mater. Today: Proc.* 2019. **6**(2):250.
47. Myronchuk V., Zmievskii Y., Dzyazko Y., Rozhdestvenska L., Zakharov V. Whey desalination using polymer and inorganic membranes: Operation conditions. *Acta Periodica Technologica.* 2018. **49**: 103.
48. Dzyazko Yu., Kolomyets E., Borysenko Yu., Chmilenco V., Fedina I. Organic-inorganic sorbents containing hydrated zirconium dioxide for removal of chromate anions from diluted solutions. *Mater. Today: Proc.* 2019. **6**(2): 260.
49. Perlova O., Dzyazko Yu., Halutska I., Perlova N., Palchik A. Anion exchange resin modified with nanoparticles of hydrated zirconium dioxide for sorption of soluble U(VI) compounds. *Springer Proc. Phys.* 2018. **210**: 3.
50. Maltseva T.V., Kolomiets E.O., Dzyazko Yu.S., Scherbakov S. Composite anion-exchangers modified with nanoparticles of hydrated oxides of multivalent metals. *Appl. Nanoscience.* 2019. **9**(5): 997.
51. Fan L., Luo C., Li X., Lu F., Qiu H., Sun M. Fabrication of novel magnetic chitosan grafted with graphene oxide to enhance adsorption properties for methyl blue. *J. Hazard. Mater.* 2012. **215**: 272.
52. Nguyen-Phan T.-D., Pham V.H., Shin F.W., Pham H.-D., Kim S., Chung J.K., Kim E.J., Hur S.H. The role of graphene oxide content on the adsorption-enhanced photocatalysis of titanium dioxide/graphene oxide composites. *Chem. Eng. J.* 2011. **170**(1): 226.
53. Cui L., Wang Y., Gao L., Hu L., Yan L., Wei Q., Du B. EDTA functionalized magnetic graphene oxide for removal of Pb(II), Hg(II) and Cu(II) in water treatment: Adsorption mechanism and separation property. *Chem. Eng. J.* 2015. **281**: 1.
54. Seredych M., Teresa J., Bandosz T.J. Reactive adsorption of hydrogen sulfide on graphite oxide/Zr(OH)₄ composites. *Chem. Eng. J.* 2011. **166**(3): 1032.
55. Dzyazko Yu.S., Rozhdestvenskaya L.M., Zmievskii Yu.G., Vilenskii A.I., Myronchuk V.G., Kornienko L.V., Vasilyuk S.V., Tsyba N.G. Organic-inorganic materials containing nanoparticles of zirconium hydrophosphate for baromembrane separation. *Nanoscale Res. Lett.* 2015. **10**: 64.
56. Sánchez-Bayo F., Goulson D., Pennacchio F., Nazzi F., Goka K., Desneux N. Are bee diseases linked to pesticides? – A brief review. *Environ. Int.* 2016. **89–90**: 7.

57. Mew E.M., Padmanathan P., Konradsen F., Eddleston M., Chang S.-S., Phillips M.R., Gunnell D. The global burden of fatal self-poisoning with pesticides 2006-15: Systematic review. *J. Affect. Disord.* 2017. **219**: 93.
58. Wood T.J., Goulson D. The environmental risks of neonicotinoid pesticides: a review of the evidence post 2013. *Environ. Sci. Pollut. Res.* 2017. **24**(21): 17285.
59. Rani M., Shanker U., Jassal V. Recent strategies for removal and degradation of persistent & toxic organochlorine pesticides using nanoparticles: A review. *J. Environ. Manag.* 2017. **190**: 208.
60. State Standard of Ukraine. (DSTU 7312:2013).
61. Interstate Standard (GOST 21.560.2-82). Mineral fertilizers. Method for determination of granules static strength.
file:///D:/2019%20%D0%A5%D1%96%D0%BC%D1%96%D1%8F%20%D1%82%D0%B0%20%D1%82%D0%B5%D1%85%D0%BD%D0%BE%D0%BB%D0%BE%D0%B3%D1%96%D1%8F%20%D0%BF%D0%BE%D0%B2%D0%B5%D1%80%D1%85%D0%BD%D1%96%D0%93%D0%9E%D0%A1%D0%A2.pdf
62. Kang Ch., Wang Y., Li R., Du Y., Li J., Zhang B., Zhou L., Du Y. A modified spectrophotometric method for the determination of trace amounts of phenol in water. *Microchem. J.* 2000. **64**(2): 161.
63. Interstate Standard (GOST 31940-2012). Drinking water. Methods for determination of sulfate content. <http://docs.cntd.ru/document/gost-31940-2012>
64. Interstate Standard (GOST 31954-2012). Drinking water. Methods of hardness determination. <http://docs.cntd.ru/document/1200097815>
65. Gregg S.J., Sing K.S.W. *Adsorption, Surface Area and Porosity*. (London: Academic Press, 1991).
66. Leboda R., Mendyk E., Gierak A., Tertykh V.A. Hydrothermal modification of silica gels (xerogels) 2. Effect of the duration of treatment on their porous structure. *Colloids Surfaces A*. 1995. **105**(2–3): 191.
67. Archie G.E. The electrical resistivity log as an aid in determining some reservoir characteristics. *Trans. AIME*. 1942. **146**(1): 1.
68. Rice R.W. *Porosity of ceramics*. (New York, Basel, Honc Kong, Marcel Dekker, 1998).
69. Rouquerol F., Rouquerol J., Sing H. *Adsorption by powders and porous solids. Principles, methodology and application*. (London, San Diego: Academic Press, 1999).
70. Dzyazko Yu.S., Palchik O.V., Ogenko V.M., Shtemberg L.Ya., Bogomaz V.I., Protsenko S.A., Khomenko V.G., Makeeva I.S., Chernysh O.V., Dzyazko O.G. Nanoporous biochar for removal of toxic organic compounds from water. *Springer Proceedings in Physics*. 2019. **222**: 209.
71. <http://www.pesticidy.ru>
72. Goncharuk V.V., Dubrovina L.V., Kucheruk D.D., Samsoni-Todorov A.O., Ogenko V.M., Dubrovin I.V. Water purification of dyes by ceramic membranes modified by pyrocarbon of carbonized polyisocyanate. *J. Water Chem. Technol.* 2016. **38**(1): 34.

Received 07.08.2019, accepted 20.11.2019